

One-Dimensional Coordination Polymers from the Self-Assembly of Copper(II) Carboxylates and 4,4′-Dithiobis(pyridine)

Ryo Horikoshi and Masahiro Mikuriya*

Department of Chemistry and Open Research Center for Coordination Molecule-besed Devices, School of Science and Technology, Kwansei Gakuin University, 2-1 Gakuen, Sanda, Hyogo 669-1337

Received August 31, 2004; E-mail: junpei@ksc.kwansei.ac.jp

A twisted ligand, 4,4′-dithiobis(pyridine), 4pds, was reacted with copper(II) carboxylates to synthesize one-dimensional coordination polymers: $[Cu_4(CH_3COO)_6(\mu_3\text{-}OH)_2(4pds)_2]_n$ (**1**), $[Cu(CH_3COO)_2(4pds)\cdot 6H_2O]_n$ (**2**), $[\{Cu_2(C_6H_5COO)_4\}_2(4pds)_2]_n$ (**3**), and $[\{Cu_2[CH_3(CH_2)_4COO]_4\}_2(4pds)_2]_n$ (**4**). The crystal structure of **1** reveals a repeated rhomboid structure in which the $Cu_4(CH_3COO)_6(OH)_2$ core is linked by two 4pds ligands. The 4:2 (Cu:4pds) stoichiometry of **1** transforms into the 1:1 (Cu:4pds) one of **2** in aqueous solution. Compound **2** has a porous honeycomb-like structure, which is occupied by carboxylate ions and water molecules. Compounds **3** and **4** are zigzag chains consisting of alternate linking of the $Cu_2(RCOO)_4$ unit and 4pds ligand. The variable-temperature magnetic susceptibility data of **1** and **3** are consistent with the net antiferromagnetic interaction within the tetranuclear or dinuclear core.

The control and design of supramolecular architectures in the solid state is an interesting theme of modern chemistry.[1–9] In particular, the topological construction of metal complexes exhibiting interesting electrochemical, magnetic, and optical properties have received much attention.[10–17] In order to construct new coordination polymers with an interesting structures and properties, we combined a disulfide-bridged pyridine, 4,4′-dithiobispyridine (4pds), with copper(II) carboxylates. The 4pds ligand has a twisted structure and accompanies the axial chirality, generating the P- and the M-forms of optical antipodes (Scheme 1). Although many coordination compounds with 4pds have been reported,[18–22] there have been few studies on their chiral derivatives. Possible structures generated from combinations of the 4pds ligand and mononuclear metal sources are chiral or achiral coordination polymers, associating with the axial chirality and bridging ability of the 4pds ligand.[23,24] Previously, Mochida and Horikoshi demonstrated that combinations of 4pds with $[M(hfac)_2]$ (M = Cu, Mn; hfac = 1,1,1,5,5,5-hexafluoroacetylacetonate) and several Ag salts produce helix, achiral zigzag chains, and chiral sheets.[23,24] In addition, macrocyclic complexes and one-dimensional coordination polymers were also obtained by combinations of 4pds with [M(hfac)] (M = Co, Ni) and zinc(II) salts.[25,26] Their structures are dramatically different from one another, showing dimensionally diverse supramolecules. On the other hand, copper(II) carboxylates, when they are combined with appropriate bridging ligands, construct coordination polymers with diverse assembled structures, because the carboxylate group shows several coordination fashions.[27–30] Further, copper(II) carboxylates are frequently employed as a spin source in supramolecular assemblies, owing to their structural diversity as well as their synthetic versatility.[27–30] Therefore, combinations of 4pds and copper(II) carboxylates are promising to produce new coordination polymers with unique structures and interesting magnetic properties.

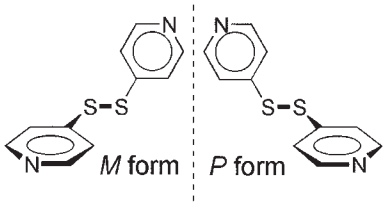

Scheme 1. Optical antipodes of 4,4′-dithiobis(pyridine) (4pds).

We report here on the synthesis and crystal structures of novel one-dimensional chains: $[Cu_4(CH_3COO)_6(\mu_3\text{-}OH)_2(4pds)_2]_n$ (**1**), $[Cu(CH_3COO)_2(4pds)\cdot 6H_2O]_n$ (**2**), $[\{Cu_2(C_6H_5COO)_4\}_2(4pds)_2]_n$ (**3**), and $[\{Cu_2[CH_3(CH_2)_4COO]_4\}_2(4pds)_2]_n$ (**4**).

Experimental

General Procedure and Chemicals. All reagents and solvents were commercially available. Infrared spectra were recorded on a JASCO MFT-2000 spectrometer as KBr pellets. Solid-state UV–vis spectra were recorded in the range of 200–1000 nm on a Shimadzu UV-3100 spectrophotometer (reflection method). Magnetic susceptibilities were measured by means of a Quantum Design MPMS-5S SQUID susceptometer in the range of 4.5–300 K at a constant field of 0.5 T. A thermogravimetric analysis was performed under a nitrogen atmosphere at a heating rate of 5 °C/min on a Seiko TG/DTA 220U, in the temperature range 25–400 °C. Elemental analyses were performed on a Thermo-Finnigan FLASH EA1112 analyzer.

X-ray Diffraction Studies. Powder X-ray measurements were performed on a Rigaku RINT 2000. X-ray diffraction data for single crystals were collected on a Bruker SMART APEX CCD diffractometer equipped with a graphite crystal and incident-beam monochromator using Mo Kα radiation ($\lambda = 0.71073$ Å) at 293 K for **1**–**3**, and 200 K for **4**. The crystal data, data-collection parameters and analysis statistics for **1**, **3**, and **4** are listed in Table 1. Selected bond angles and bond lengths are given in Table 2. The frames were integrated using the Siemens

Published on the web May 6, 2005; DOI 10.1246/bcsj.78.827

Table 1. Crystallographic Data for **1**, **3**, and **4**

	1	**3**	**4**
Empirical formula	$C_{32}H_{36}Cu_4N_4O_{14}S_4$	$C_{38}H_{28}Cu_2N_2O_8S_2$	$C_{68}H_{104}Cu_4N_4O_{16}S_4$
Formula weight	1083.05	831.86	1615.95
Temperature/K	296	296	200
Crystal dimensions/mm^3	$0.5 \times 0.2 \times 0.2$	$0.2 \times 0.1 \times 0.1$	$0.6 \times 0.4 \times 0.2$
Crystal system	monoclinic	triclinic	monoclinic
Space group	$P2_1/n$ (No. 14)	$P\bar{1}$ (No. 2)	$P2_1/c$ (No. 14)
a/Å	12.540(2)	10.4232(19)	14.832(3)
b/Å	18.647(3)	10.9518(19)	21.306(5)
c/Å	18.254(3)	17.478(3)	24.678(6)
α/°	90	72.098(3)	90
β/°	104.523(3)	87.542(3)	99.075(4)
γ/°	90	87.012(3)	90
V/Å^3	4132.1(11)	1895.2(6)	7701(3)
Z	4	2	4
d_{calcd}/g cm^{-3}	1.741	1.458	1.394
μ/mm^{-1}	2.301	1.285	1.262
Diffractometer	Bruker SMART APEX CCD	Bruker SMART APEX CCD	Bruker SMART APEX CCD
No. of reflection	9536	8308	17481
No. of observation	7199	5924	11487
Refl./Parameter ratio	12.5	11.9	13.2
$R1$, $wR2[I > 2\sigma(I)]$[a)]	0.0339, 0.0846	0.0406, 0.1109	0.0500, 0.1164
Goodness-of-fit on F^2	1.003	1.004	0.990

a) $R1 = \Sigma||F_o| - |F_c||/\Sigma|F_o|$; $R_w = [\Sigma w(F_o^2 - F_c^2)^2/\Sigma w(F_o^2)^2]^{1/2}$.

SAINTPLUS[31] software package, and the data were corrected for absorption using the SADABS[32] program. The structures were solved by the direct method (SHELXS 97[33]) and expanded using Fourier techniques. The non-hydrogen atoms were refined anisotropically. The hydrogen atoms attached to carbon atoms were inserted at the calculated positions and allowed to ride on their respective parent atoms. The hydrogen atoms attached to oxygen atoms were located in electron-density maps and refined at fixed distances from the respective parent atoms.

CCDC 220149 (**1**), CCDC 220150 (**3**), and CCDC 223059 (**4**) contain supplementary crystallographic data for this paper. These data can be obtained free of charge at www.ccdc.cam.ac.uk/conts/retrieving.html [or from the Cambridge Crystallographic Data Centre, 12 Union Road, Cambridge CB12 1EZ, UK; fax: (internat.) +44-1223/336-033; E-mail: deposit@ccdc.cam.ac.uk].

Synthesis of $[Cu_4(CH_3COO)_6(\mu_3\text{-}OH)_2(4pds)_2]_n$ (1). To a methanol solution (0.5 mL) of 4pds (11 mg, 5×10^{-5} mol), a solution of $Cu_2(CH_3COO)_4 \cdot H_2O$ (19 mg, 5×10^{-5} mol) in methanol (3 mL) was added, forming a pale-green precipitate. After the reaction mixture was stirred for 1 h, the solid was filtered off and washed with methanol (3×5 mL). The pale-green solid was recrystallized form DMF/diethyl ether (1:3 v:v) to give compound **1** as a pale-green solid (21 mg, 61%). X-ray quality crystals were grown by slow evaporation of a DMF solution at ambient temperature. Found: C, 35.48; H, 3.50; N, 5.30%. Calcd for $C_{32}H_{36}Cu_4N_4O_{14}S_4$: C, 35.49, H, 3.35; N, 5.17%. IR (KBr): 3102, 3053, 3026, 2920, 2467, 2062, 1558, 1484, 1396, 1336, 1223, 1070, 1028, 914, 863, 816, 716, 668, and 616 cm^{-1}. UV–vis (solid-state): λ_{max} 219, 259, 374, and 715 nm.

Synthesis of $[Cu(CH_3COO)_2(4pds) \cdot 6H_2O]_n$ (2). Compound **1** (33 mg, 3×10^{-5} mol) was recrystallized from distilled water to give compound **2** as a blue crystalline solid (8 mg, 27%). X-ray quality crystals were grown by slow evaporation of an aqueous solution at ambient temperature. Found: C, 33.37; H, 4.94; N, 5.49%. Calcd for $C_{14}H_{26}CuN_2O_{10}S_2$: C, 32.97; H, 5.14; N, 5.49%. IR (KBr): 3393, 3060, 2462, 1589, 1476, 1412, 1344, 1314, 1213, 1057, 844, 799, 715, and 681 cm^{-1}.

Synthesis of $[\{Cu_2(C_6H_5COO)_4\}_2(4pds)_2]_n$ (3). Compound **3** was prepared as for **1** using 4pds (22 mg, 1×10^{-4} mol) and $Cu_2(C_6H_5COO)_4$ (61 mg, 1×10^{-4} mol). A blue solid was obtained in 37% yield (31 mg). X-ray quality crystals were grown by slow evaporation of a DMF solution at ambient temperature. Found: C, 54.92; H, 3.70; N, 3.39%. Calcd for $C_{76}H_{56}Cu_4N_4O_{16}S_4$: C, 54.87; H, 3.39; N, 3.37%. IR (KBr): 3064, 3025, 1637, 1573, 1482, 1405, 1221, 1175, 1066, 1025, 844, 811, 715, and 687 cm^{-1}. UV–vis (solid-state): λ_{max} 219, 303, 374(sh), and 709 nm.

Synthesis of $[\{Cu_2[CH_3(CH_2)_4COO]_4\}_2(4pds)_2]_n$ (4). Compound **4** was prepared as for **1** using 4pds (22 mg, 1×10^{-4} mol) and $[Cu_2\{CH_3(CH_2)_4COO\}_4]$ (68 mg, 1×10^{-4} mol). A blue solid was obtained in 56% yield (50 mg). X-ray quality crystals were grown by slow evaporation of a methanol solution at ambient temperature. Found: C, 50.28; H, 6.51; N, 3.30%. Calcd for $C_{68}H_{104}Cu_4N_4O_{16}S_4$: C, 50.54; H, 6.49; N, 3.47%. IR (KBr): 2956, 2928, 2856, 1617, 1581, 1418, 1319, 1222, 807, and 709 cm^{-1}. UV–vis (solid-state): λ_{max} 211, 266, 380, and 714 nm.

Results and Discussion

Synthesis of One-dimensional Coordination Polymers (1–4). The general reaction schemes are shown in Scheme 2. Combinations of 4pds and copper(II) carboxylates form coordination polymers with a one-dimensional chain structure: $[Cu_4(CH_3COO)_6(\mu_3\text{-}OH)_2(4pds)_2]_n$ (**1**), $[Cu(CH_3COO)_2(4pds) \cdot 6H_2O]_n$ (**2**), $[\{Cu_2(C_6H_5COO)_4\}_2(4pds)_2]_n$ (**3**), and $[\{Cu_2[CH_3(CH_2)_4COO]_4\}_2(4pds)_2]_n$ (**4**). Satisfactory analytical data were obtained for the present complexes. The treatment of $Cu(CH_3COO)_2 \cdot H_2O$ with 4pds afforded a pale-

Table 2. Selected Bond Distances (Å) and Angles (°), with esds in Parentheses for **1**, **3**, and **4**

1			
Cu(1)–N(1)	2.003(2)	Cu(1)–O(1)	1.976(2)
Cu(1)–O(3B)	1.970(5)	Cu(1)–O(4A)	2.032(4)
Cu(1)–O(5)	2.245(2)	Cu(1)–O(7)	1.960(2)
Cu(2)–N(2)	1.988(2)	Cu(2)–O(6)	1.943 (2)
Cu(2)–O(7)	1.955(2)	Cu(2)–O(8)	1.996(2)
Cu(3)–N(3)	1.990(2)	Cu(3)–O(7)	1.992(2)
Cu(3)–O(8)	1.946 (2)	Cu(3)–O(9)	1.932(2)
Cu(4)–N(4)	2.028(2)	Cu(4)–O(8)	1.985(2)
Cu(4)–O(10)	2.227 (2)	Cu(4)–O(11A)	1.978(2)
Cu(4)–O(12B)	1.998(2)	Cu(4)–O(13)	1.968(2)
S(1)–S(2)	2.0284(1)	S(3)–S(4)	2.023(1)
Cu(1)–O(7)–Cu(2)	105.04(8)	Cu(2)–O(7)–Cu(3)	99.31(7)
Cu(3)–O(7)–Cu(1)	113.41(9)	Cu(3)–O(8)–Cu(4)	104.98(8)
Cu(2)–O(8)–Cu(3)	99.48(7)	Cu(4)–O(8)–Cu(2)	115.49(8)
3			
Cu(1)–N(1)	2.185(2)	Cu(1)–O(1)	1.964(2)
Cu(1)–O(2)	1.961(2)	Cu(1)–O(3)	1.980(2)
Cu(1)–O(4)	1.964(2)	Cu(2)–N(2)	2.166(2)
Cu(2)–O(5)	1.974(2)	Cu(2)–O(6)	1.986(2)
Cu(2)–O(7)	1.952(2)	Cu(2)–O(8)	1.954(2)
S(1)–S(2)	2.019(1)		
4			
Cu(1)–N(1)	2.181(3)	Cu(1)–O(1)	1.960(3)
Cu(1)–O(3)	1.979(3)	Cu(1)–O(5)	1.954(2)
Cu(1)–O(7)	1.980(3)	Cu(2)–N(3)	2.180(3)
Cu(2)–O(2)	1.959(3)	Cu(2)–O(4)	1.962(3)
Cu(2)–O(6)	1.963(3)	Cu(2)–O(8)	1.960(3)
Cu(3)–N(4)	2.182(3)	Cu(3)–O(9)	1.966(2)
Cu(3)–O(11)	1.964(2)	Cu(3)–O(13)	1.958(2)
Cu(3)–O(15)	1.966(2)	Cu(4)–N(2)	2.182(3)
Cu(4)–O(10)	1.940(2)	Cu(4)–O(12)	1.983(3)
Cu(4)–O(14)	1.942(2)	Cu(4)–O(16)	1.972(2)
S(1)–S(2)	2.022(2)	S(3)–S(4)	2.022(2)

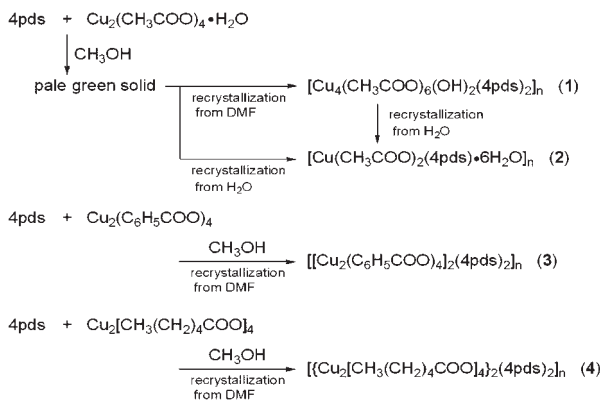

Scheme 2. General reaction schemes.

green solid. Recrystallization of the pale-green solid from DMF gave compound **1**, while that from aqueous solution afforded compound **2**. Even though the powder X-ray diffraction pattern of the initial pale green product was somewhat similar to that of **2**, which was calculated using the single-crystal X-ray data, they were not the same. The crystal structure of **1** contains a μ_3-OH-bridged tetranuclear core (vide infra). The formation of such a novel tetranuclear core may have occurred in the presence of a small amount of water molecules, which must be the origin of the hydroxo groups. The 4:2 (Cu:4pds) stoichiometry of **1** transforms into the 1:1 (Cu:4pds) one of compound **2** in aqueous solution. An attempt was first made to synthesize a coordination polymer by combining an anhydrous $Cu(CH_3COO)_2$ with 4pds in absolute DMF under an argon atmosphere. This procedure afforded an air-sensitive green powder, which was suggested to be $[Cu_2(CH_3COO)_2(CH_3O)_2(4pds)]$, in which the $Cu_2(CH_3COO)_2(CH_3O)_2$ paddle wheel units may be linked by 4pds ligands.[34] The treatment of $Cu(C_6H_5COO)_2$ with 4pds afforded compound **3**. Similarly, a treatment of $Cu\{CH_3(CH_2)_4COO\}_2$ with 4pds gave compound **4**. Other copper(II) carboxylates, such as $Cu(HCOO)_2$, $Cu(CF_3COO)_2$, $Cu(CH_3CH_2COO)_2$, and $Cu\{CH_3(CH_2)_n COO\}_2$ ($n = 5$–7), were also examined. However, these carboxylates did not form crystalline materials with 4pds, except for the cases of $Cu\{CH_3(CH_2)_nCOO\}_2$ ($n = 2$ and 3), where microcrystalline precipitates, which are not suitable for single-crystal X-ray analysis, formed.

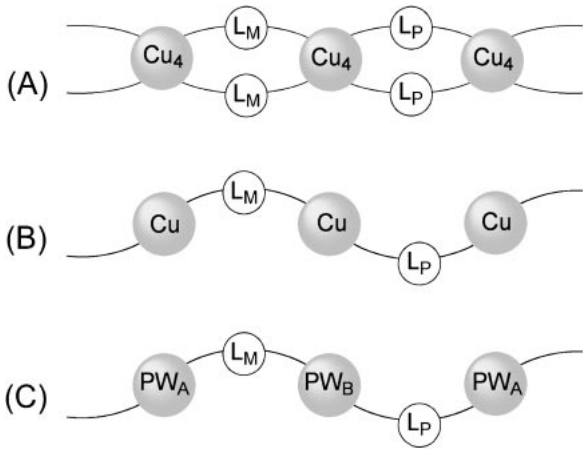

Scheme 3. Schematic illustration of zigzag chain structure in the present compounds: (A) for **1**, (B) for **2**, and (C) for **3** and **4**: Letters L_P and L_M represent two optical antipodes of the 4pds ligand with P-form and M-form, respectively. The letters "Cu_4", "Cu", and "PW" represent "$Cu_4(CH_3COO)_6(OH)_2$", "$Cu(CH_3COO)_2$", and "$Cu_2(RCOO)_4$ ($R = C_6H_5$, $CH_3(CH_2)_4$)" units, respectively.

From the viewpoint of chirality, the present compounds consist of alternated linkages of different optical antipodes of the 4pds ligands and the copper(II) carboxylate unit (Scheme 3). Therefore, compounds **1**–**4** have an achiral structure with a centrosymmetric space group. We can expect possible structures of a one-dimensional chain resulting from combinations with 4pds that are achiral zigzag chain, achiral repeated rhomboid, chiral helix, and chiral repeated rhomboid.[23] Compound **1** is classified as an achiral repeated rhomboid, while compounds **2**–**4** are achiral zigzag chains.

A Repeated Rhomboid $[Cu_4(CH_3COO)_6(\mu_3\text{-}OH)_2(4pds)_2]_n$ (1). Compound **1** assumes a one-dimensional repeated rhomboid, as shown in Fig. 1, which is composed of an alternate linking of one $Cu_4(CH_3COO)_6(OH)_2$ core and

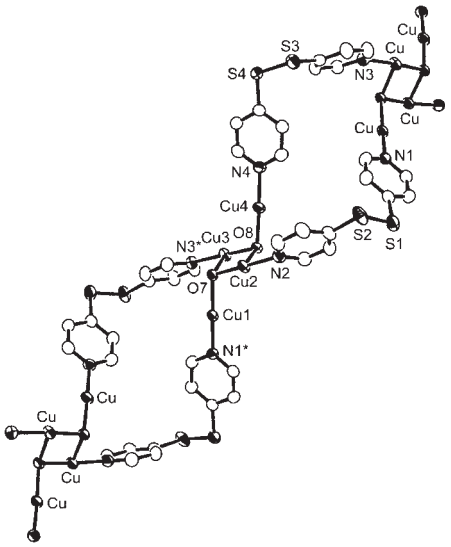

Fig. 1. Repeated rhomboid structure in **1**. Hydrogen atoms and CH_3COO groups are omitted for clarity.

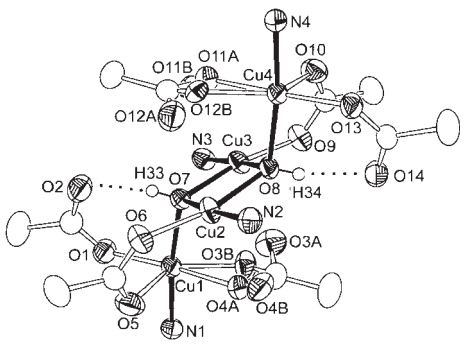

Fig. 2. ORTEP[42] drawing of **1** with the atom numbering scheme, showing coordination environment around the $Cu_4(CH_3COO)_6(OH)_2$ core. Displacement ellipsoids are shown at the 50% probability level. Hydrogen atoms are omitted for clarity. Letters A and B represent the disordered moieties of carboxylato groups. Dashed lines indicate hydrogen bonds.

two 4pds ligands. The repeated rhomboid runs along the [1,0,1] direction, involving a crystallographic 2-fold screw axis. There are no significant inter-chain interactions in the crystal. The coordination environments around the copper(II) ions in **1** are shown in Fig. 2. There are four crystallographically independent copper atoms in **1**, in which the coordination environments of the Cu(1) and Cu(2) atoms are very similar to those of the Cu(4) and Cu(3) atoms, respectively. The Cu(1) and Cu(4) atoms are bound to three carboxylate oxygen atoms, a hydroxo oxygen atom and a pyridine nitrogen atom in a distorted square pyramidal configuration, while the Cu(2) and Cu(3) atoms are surrounded by a carboxylato oxygen atom, two hydroxo oxygen atoms, and a pyridine nitrogen atom in a distorted square configuration. The hydroxo oxygen atoms, O(7) and O(8), link three copper(II) ions in a μ_3 fashion to construct two $Cu_3(O)H$ tetrahedron units that share the Cu(2)···Cu(3) edge. Interestingly, intra-molecular hydrogen bonds were observed between the hydroxo group and the bridged carboxylato, O(2)···H(33)–O(7) (2.617 Å) and O(14)···H(34)–O(8) (2.672 Å), which may prevent a disordering of the carboxylato groups. The Cu–O(H) distances and Cu–O(H)–Cu′ angles around the μ_3-hydroxo groups are comparable to those found in the discrete molecular complex $[Cu_4(oct)_6(OH)_2(4\text{-apy})_2]$ (oct = octanoate, 4-apy = 4-aminopyridine).[35] The Cu(2)···Cu(3) distance is 3.0086(6) Å.

In complex **1**, three types of carboxylato groups are present; of these one bridges from the axial position (O5) of Cu(1) to the equatorial position (O6) of Cu(2); likewise for Cu(4) and Cu(3), respectively. The second is bound as a monodentate ligand at the equatorial position (O4A, O3B, O11A, or O12B) of Cu(1) and Cu(4), in which oxygen atoms of the carboxylato groups are disordered with a site occupancy ratio of ca. 5:5 and 9:1, respectively. The third one is not only bound as a monodentate ligand in the equatorial position O1(O13) of Cu1(Cu4), but also hydrogen bonded to the hydroxo group O7(O8), forming a six-membered ring: Cu(1)–O(1)–C(11)–O(2)–H(33)–O(7) (Cu(4)–O(13)–C(21)–O(14)–H(34)–O(8)).

The infrared spectra of **1** display strong bands at 1680–1560, 1470–1380, and 1336 cm^{-1}, which are attributable to ν(COO). A thermogravimetric analysis of **1** showed a single sharp weight loss between 153–239 °C of 38.7% of the original weight, corresponding to a loss of the two 4pds ligands (calcd 40.7%). Around and above 250 °C, a TG trace of **1** gradually decreases with increasing temperature. These results are consistent with the crystal structure of **1**. Magnetic-susceptibility measurements were made in the temperature range of 4.5–300 K (Fig. 3). At 300 K, the effective magnetic moment is 2.30 μ_B, which is much smaller than that expected for a magnetically isolated four copper(II) $S = 1/2$ ions (theoretical value for $g = 2$, $\mu_{eff} = 3.46\ \mu_B$). This curve is characteristic of an antiferromagnetic interaction between the copper(II) ions. On the basis of the crystal structure (Fig. 2), the data were fit to a Heisenberg Hamiltonian for a tetranuclear model,

$$H = -2J_1(S_{Cu1}\cdot S_{Cu2} + S_{Cu3}\cdot S_{Cu4}) - 2J_2(S_{Cu2}\cdot S_{Cu3}) - 2J_3(S_{Cu1}\cdot S_{Cu3} + S_{Cu2}\cdot S_{Cu4}) - 2J_4(S_{Cu1}\cdot S_{Cu4}), \quad (1)$$

where J_1 describes the nearest-neighbor interaction between the outer pairs of copper ions, J_2 the nearest-neighbor interaction between the central pair of copper ions, J_3 the next-nearest neighbor interactions, and J_4 the interaction between the terminal two copper ions.[36] The J_1, J_2, and J_3 constants correspond to μ-hydroxo/μ-acetato, di-μ-hydroxo, and μ-hydroxo

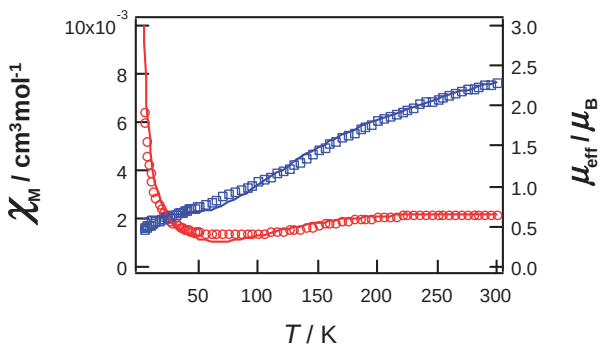

Fig. 3. Temperature dependence of magnetic susceptibility (○) and effective magnetic moment (□) for **1**. Solid lines represent the fit described in the text.

bridges, respectively. The experimental susceptibility data were fit to the van-Vleck equation based on the Heisenberg Hamiltonian (1):

$$\chi_M = (1-p)(N\mu_B{}^2 g^2/kT)[10\exp(-E_1/kT) + 2\exp(-E_2/kT) + 2\exp(-E_3/kT) + 2\exp(-E_4/kT)]/[5\exp(-E_1/kT) + 3\exp(-E_2/kT) + 3\exp(-E_3/kT) + 3\exp(-E_4/kT) + \exp(-E_5/kT) + \exp(-E_6/kT)] + pN\mu_B{}^2 g^2/kT + 4N\alpha, \quad (2)$$

where $E_1 = -J_1 - (1/2)J_2 - J_3 - (1/2)J_4$, $E_2 = J_1 - (1/2)J_2 + J_3 - (1/2)J_4$, $E_3 = (1/2)(J_2 + J_4) + [(J_2 - J_4)^2 + (J_3 - J_1)^2]^{1/2}$, $E_4 = (1/2)(J_2 + J_4) - [(J_2 - J_4)^2 + (J_3 - J_1)^2]^{1/2}$, $E_5 = J_1 + J_3 + (1/2)(J_2 + J_4) + [4(J_1{}^2 + J_3{}^2) + J_2{}^2 + J_4{}^2 - 2J_1(J_2 + 2J_3 + J_4) - 2J_2(J_3 - J_4) - 2J_3J_4]^{1/2}$, $E_6 = J_1 + J_3 + (1/2)(J_2 + J_4) - [4(J_1{}^2 + J_3{}^2) + J_2{}^2 + J_4{}^2 - 2J_1(J_2 + 2J_3 + J_4) - 2J_2(J_3 - J_4) - 2J_3J_4]^{1/2}$, p = fraction of mononuclear impurity, and $N\alpha$ = temperature-independent paramagnetism which was set to 60×10^{-6} cm^3 mol^{-1} for each copper atom.[37] By using equation (2), a satisfactory fit of the experimental data was obtained with the following parameters: $J_1 = -182$ cm^{-1}, $J_2 = -258$ cm^{-1}, $J_3 = -184$ cm^{-1}, $J_4 = -117$ cm^{-1}, $p = 0.027$, and $g = 2.1$ (fixed) (Fig. 3). The most efficient exchange pathway in **1** is that corresponding to J_2: two copper(II) ions bridged by two hydroxo-oxygen atoms. Therefore, it is reasonable to assume that the magnetic coupling is mainly dominated by the strongest interaction J_2, although the magnitude of the J_2 value is rather high considering Hatfield's relationship between the $2J$ value and the Cu–O–Cu angle for the di-μ-hydroxo-bridged copper(II) dimer.[38]

A Porous One-dimensional Architecture of $[Cu(CH_3COO)_2(4pds)\cdot 6H_2O]_n$ (2).

In contrast to **1**, compound **2** has a porous honeycomb-like architecture, although its local structure is a simple zigzag chain (Fig. 4). Compound **2** consists of two zigzag chains that run along the [0,1,1] and [0,−1,1] directions, respectively, and cross perpendicular to each other. The honeycomb-like channel is occupied by guest water molecules and carboxylate ions that are highly disordered at room temperature. The size of the honeycomb-like cavity in **2** is ca. 12 Å (Cu···Cu distance) by ca. 16 Å (S···S distance). Unfortunately, despite many attempts, we failed to obtain a satisfactory quality of crystallographic data, and therefore a more detailed analysis of the structure of **2** could not be performed.[39] From the preliminary X-ray crystal structure, we speculate that the copper(II) ions in **2** should adopt a square–planar environment and be bound to two carboxylato groups and two pyridyl nitrogen atoms of the 4pds ligands. The crystal of **2** gradually releases the guest water molecules at room temperature. After drying, compound **2** is decomposed and becomes insoluble in water.

A thermogravimetric analysis of **2** shows two single weight losses between 30–76 °C of 21.5% and 160–230 °C of 42.5% of the original weight, corresponding to a loss of the $6H_2O$ (calcd 21.2%) and the 4pds ligand (calcd 43.1%), respectively. In the range of 250–400 °C, the TG trace of **2** gradually decreases with increasing temperature. From the thermogravimetric data of **1** and **2**, it can be seen that 4pds moieties are released at around 200 °C. Since the starting material of $Cu_2(CH_3COO)_4\cdot H_2O$ decomposes at around 240 °C, the weight losses of **1** and **2** around 250 °C correspond to the thermal decomposition of $Cu_4(CH_3COO)_6(OH)_2$ and $Cu(CH_3COO)_2$ units, respectively.

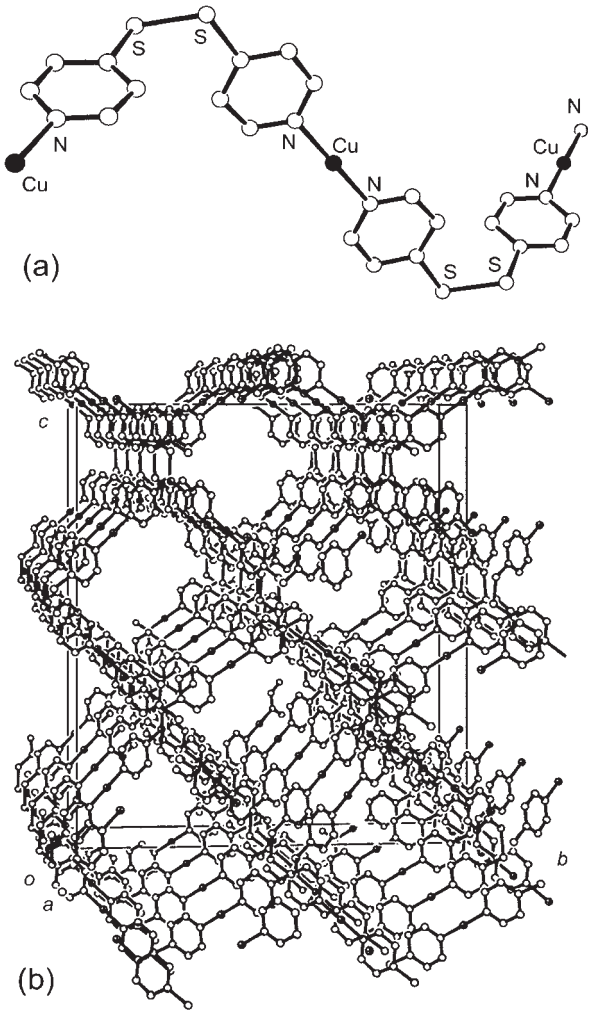

Fig. 4. (a) Zigzag chain structure in **2**. (b) Packing diagram of **2** viewed along the *a* axis. Hydrogen atoms, carboxylic groups, and guest water molecules are omitted for clarity. Copper ions are shaded.

Simple Zigzag Chains $[\{Cu_2(C_6H_5COO)_4\}_2(4pds)_2]_n$ (3) and $[\{Cu_2[CH_3(CH_2)_4COO]_4\}_2(4pds)_2]_n$ (4). Compounds **3** and **4** consist of alternate linking of a $Cu_2(RCOO)_4$ ($R = C_6H_5$, $CH_3(CH_2)_4$) unit and a 4pds ligand to construct simple zigzag chains, as shown in Figs. 5 and 6, respectively. The chain runs along the [1,0,1] direction for **3** and the [0,0,1] direction for **4**, respectively. On the basis of the present results, it can be presumed that the aromatic ring and alkyl chain of carboxylate moiety of **3** and **4** are suitable to occupy the interstice of the zigzag chains (vide supra). The coordination environments around the copper(II) ions in **3** and **4** are shown in Figs. 7 and 8, respectively. For complex **3**, there are two crystallographically independent copper(II) ions, Cu(1) and Cu(2). Both copper(II) ions are surrounded by a pyridine nitrogen and four carboxylato oxygen atoms to construct a distorted square

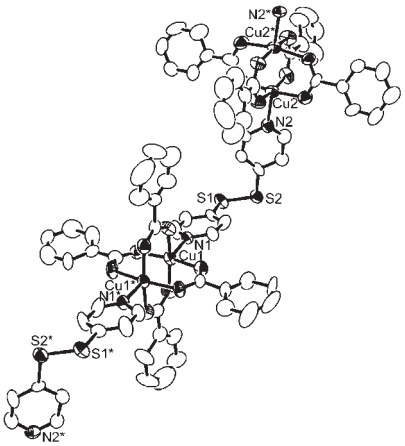

Fig. 5. Simple zigzag chain in **3**. Hydrogen atoms are omitted for clarity.

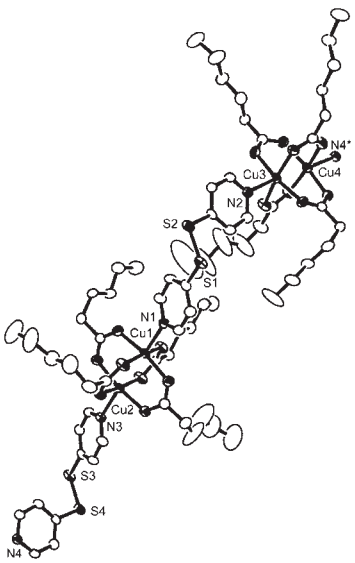

Fig. 6. Simple zigzag chain in **4**. Hydrogen atoms are omitted for clarity.

pyramidal geometry. Although the coordination environments around the crystallographically independent paddle wheel units in **3** are similar to each other, the angles between the paddle-wheel units and the pyridine moieties are slightly different. The two pyridine rings that coordinate to Cu(1) are nearly parallel to the O(1)···O(2)···O(1*)···O(2*) plane with a dihedral angle of 7.5°, while those coordinate to Cu(2) are tilted to the O(5)···O(6)···O(5*)···O(6*) plane with a dihedral angle of 36.9°. The Cu(1)···Cu(1*) and Cu(2)···Cu(2*) distances are 2.6327(8) and 2.6176(8) Å, respectively. There are four crystallographically independent copper(II) ions: Cu(1), Cu(2), Cu(3), and Cu(4), in **4**. All of them are surrounded by a pyridine nitrogen and four carboxylato oxygen atoms to construct a distorted square-pyramidal geometry. In contrast to **3**, each pyridine ring in **4** is tilted with respect to the paddle-wheel units of the O(1)···O(2)···O(6)···O(5) and O(9)···O(10)···O(14)···O(13) planes with dihedral angles of ca. 31 and 35°, respectively. The Cu(1)···Cu(2) and Cu(3)···Cu(4) distances of 2.6160(7) and 2.5969(7) Å for **4** are typical values for copper(II) paddle-wheel compounds.[27,28,40] The elongation of the Cu–N bond distances of 2.1–2.2 Å in **3** and **4** relative to the typical Cu–N value (ca. 2.0 Å) is due to a Jahn–Teller distortion of copper(II) ion; similar elongations are observed in related chain compounds of copper(II) carboxylates.[27,28]

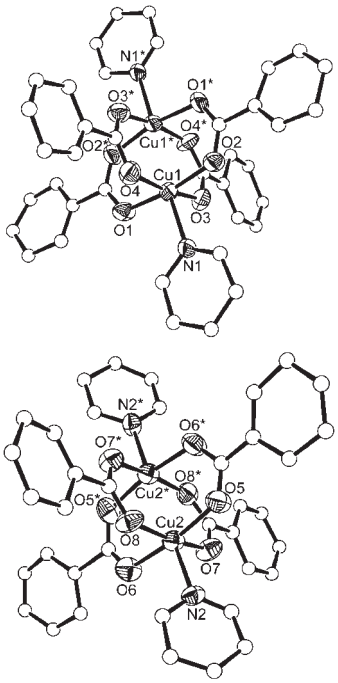

Fig. 7. ORTEP drawing of **3** with the atom numbering scheme, showing coordination environment around the $Cu_2(C_6H_5COO)_4$ paddle wheel units. Displacement ellipsoids are shown at the 50% probability level. Hydrogen atoms are omitted for clarity.

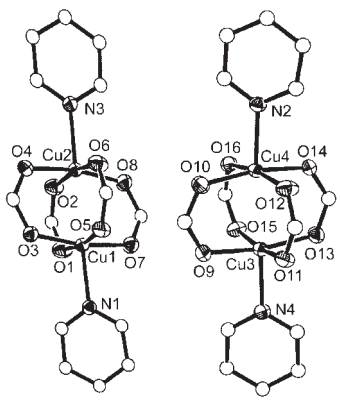

Fig. 8. ORTEP drawing of **4** with the atom numbering scheme, showing coordination environment around the $Cu_2\{CH_3(CH_2)COO\}_4$ paddle wheel unit. Displacement ellipsoids are shown at the 50% probability level. Alkyl chains and hydrogen atoms are omitted for clarity.

Thermogravimetric data of **3** and **4** exhibit weight losses between 210 and 300 °C, which are assignable to a loss of the 4pds ligand and a decomposition of the $Cu_2(RCOO)_4$ unit ($R = C_6H_5$, $CH_3(CH_2)_4$). For comparison purpose, we also measured thermogravimetric data of $Cu_2(RCOO)_4 \cdot H_2O$ ($R = C_6H_5$, $CH_3(CH_2)_4$), which show a weight loss of around

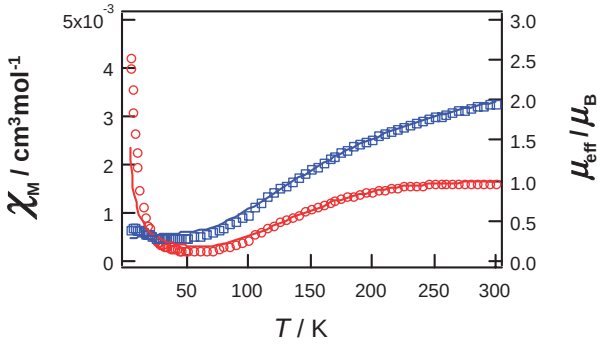

Fig. 9. Temperature dependence of magnetic susceptibility (○) and effective magnetic moment (□) for **3**. Solid lines represent the fit described in the text.

260–270 °C. Magnetic-susceptibility measurements were performed for **3**. As shown in Fig. 9, the effective magnetic moment at 300 K of **3** of 1.97 μ_B is lower than the spin-only value for two magnetically isolated copper(II) $S = 1/2$ ions ($g = 2$, $\mu_{eff} = 2.45\ \mu_B$), which indicates the presence of an antiferromagnetic interaction between the two copper(II) ions. The magnetic data were analyzed by the Bleaney–Bowers equation based on the Heisenberg model, $H = -2JS_{Cu} \cdot S_{Cu*}$

$$\chi_M = (1-p)(2N\mu_B{}^2g^2/3kT)[1 + (1/3)\exp(-2J/kT)]^{-1} + pN\mu_B{}^2g^2/2kT + 2N\alpha, \quad (3)$$

where J is an exchange coupling constant for the two copper(II) ions, p is the fraction of mononuclear impurity, and $N\alpha$ is the temperature-independent paramagnetism, which was set to 60×10^{-6} cm^3 mol^{-1} for each copper atom.[37] The best-fitting parameters are $g = 2.18$, $J = -166$ cm^{-1}, and $p = 0.011$ (Fig. 9). The obtained $2J$ value is comparable to those found in dinuclear copper(II) benzoate and its adduct.[28,41]

Conclusion

We have established the synthesis of topologically interesting coordination polymers with copper(II) carboxylates and disulfide bridged pyridine, along with magnetic measurements and thermal analysis. The 4pds ligand in assembled structures maintained its characteristic twisted conformation. The S–S distances and C–S–S–C torsion angles of the 4pds ligand in compounds **1**, **3**, and **4** are comparable to those found in $[M(hfac)_2(4pds)]_n$ (M = Cu, Mn) and $[AgX \cdot 4pds]_n$ (X = PF_6^-, ClO_4^-, OTs^-, NO_3^-).[23,24] Although compounds **1**–**4** are classified into one-dimensional chains, the local structures around the metal centers are quite different from each other. This work demonstrates that the coordination environments around the metal ions, as well as the recrystallizing solvent, play important roles in determining the extended structures of the coordination polymers. So far, chiral crystals of the coordination polymer with pds have not been isolated. All of the isolated compounds contain the racemic components of 4pds. The introduction of chiral guests or chiral metal sources may achieve an optical resolution of 4pds complexes.

We thank Prof. Tomoyuki Mochida (Toho University) for his helpful discussion. We also thank Dr. Takanori Kotera (Kao Corporation) for his help in analyzing magnetic susceptibility data. We acknowledge Mr. Hiroshi Yoshioka (Kwansei Gakuin University) for his help in the powder X-ray analysis.

References

1 "Supramolecular Chemistry, Concept and Perspectives," ed by J.-M. Lehn, Wiley-VCH, Weinheim (1995).
2 J. L. Atwood and L. J. Barbour, *Cryst. Growth Des.*, **3**, 3 (2002).
3 C. V. K. Sharma, *Cryst. Growth Des.*, **3**, 465 (2002).
4 G. F. Swiegers and T. J. Malefetse, *Coord. Chem. Rev.*, **225**, 91 (2002).
5 B. Moulton and M. J. Zaworotko, *Chem. Rev.*, **101**, 1629 (2001).
6 M. J. Zaworotko, *Chem. Commun.*, **2001**, 1.
7 S. Leininger, B. Olenynk, and P. J. Stang, *Chem. Rev.*, **100**, 853 (2000).
8 M. Munakata, L.-P. Wu, and T. Kuroda-Sowa, *Adv. Inorg. Chem.*, **46**, 173 (1999).
9 P. J. Hagrman, D. Hagrman, and J. Zubieta, *Angew. Chem., Int. Ed.*, **38**, 2638 (1999).
10 C. Janiak, *J. Chem. Soc., Dalton Trans.*, **2003**, 2781.
11 R. Horikoshi, M. Ueda, and T. Mochida, *New J. Chem.*, **27**, 933 (2003).
12 R. Horikoshi, T. Mochida, and H. Moriyama, *Inorg. Chem.*, **41**, 3017 (2002).
13 R. Horikoshi, T. Mochida, R. Torigoe, and Y. Yamamoto, *Eur. J. Inorg. Chem.*, **2002**, 3197.
14 G. Baum, E. C. Constable, D. Fenske, C. E. Housecroft, and T. Kulke, *Chem.—Eur. J.*, **5**, 1862 (1999).
15 J. S. Miller, A. J. Epstein, and W. M. Reiff, *Acc. Chem. Res.*, **21**, 114 (1988).
16 I. S. Lee, D. M. Shin, and Y. K. Chung, *Cryst. Growth Des.*, **3**, 493 (2003).
17 D. M. Shin, Y. K. Chung, and I. S. Lee, *Cryst. Growth Des.*, **2**, 521 (2002).
18 X.-Y. Yu, M. Maekawa, T. Morita, H.-C. Chang, S. Kitagawa, and G.-X. Jin, *Bull. Chem. Soc. Jpn.*, **75**, 267 (2002).
19 A. J. Blake, N. R. Brooks, N. R. Champness, M. Crew, A. Deveson, D. Fenske, D. H. Gregory, L. R. Hanton, P. Hubberstey, and M. Schröder, *Chem. Commun.*, **2001**, 1432.
20 F. M. Tabellion, S. R. Seidel, A. M. Arif, and P. J. Stang, *J. Am. Chem. Soc.*, **123**, 7740 (2001).
21 M. Kondo, M. Shimamura, S. Noro, Y. Kimura, K. Uemura, and S. Kitagawa, *J. Solid State Chem.*, **152**, 113 (2000).
22 J. Luo, M. Hong, R. Wang, D. Yuan, R. Cao, L. Han, Y. Xu, and Z. Lin, *Eur. J. Inorg. Chem.*, **2003**, 3623.
23 R. Horikoshi, T. Mochida, N. Maki, S. Yamada, and H. Moriyama, *J. Chem. Soc., Dalton Trans.*, **2002**, 28.
24 R. Horikoshi, T. Mochida, and H. Moriyama, *Inorg. Chem.*, **40**, 2430 (2001).
25 R. Horikoshi, T. Mochida, K. Kurihara, and M. Mikuriya, *Cryst. Growth Des.*, **5**, 243 (2005).
26 R. Horikoshi and M. Mikuriya, *Cryst. Growth Des.*, **5**, 223 (2005).
27 M. Mikuriya, R. Nukada, H. Morishita, and M. Handa, *Chem. Lett.*, **1995**, 617.
28 R. Nukada, W. Mori, S. Takamizawa, M. Mikuriya, M. Handa, and H. Naono, *Chem. Lett.*, **1999**, 367.
29 M. Mikuriya, H. Azuma, and M. Handa, *Mol. Cryst. Liq. Cryst.*, **342**, 205 (2000).
30 M. Mikuriya, H. Azuma, and M. Handa, *Mol. Cryst. Liq.*

Cryst., **379**, 205 (2002).

31 SAINTPLUS: "Program package for area detector absorption correction," Siemens Analytical X-Ray Instruments Inc., Madison, WI (1994–1996).

32 SADABS: "Program in the SHELXL-97 software."

33 G. M. Sheldrick, "Program for the Solution of Crystal Structures," University of Göttingen, Germany (1997).

34 $C_{16}H_{20}Cu_2N_2O_6S_2$ = $[Cu_2(CH_3COO)_2(CH_3O)_2(4pds)]$ (1055.13): calcd: C, 36.43; H, 3.82; N, 5.31%. found: C, 36.04; H, 3.91; N, 5.72%. IR (KBr disc): 3094 (m), 3056 (m), 1626 (s), 1585 (s), 1483 (m), 1439 (s), 1224 (s), 1065 (m), 1015 (m), 827 (m), 710 (m), and 684 (s) cm^{-1}.

35 N. Lah, J. Koller, G. Giester, P. Segedin, and I. Leban, *New J. Chem.*, **26**, 933 (2002).

36 B. Chiari, O. Piovesana, T. Tarantelli, and P. F. Zanazzi, *Inorg. Chem.*, **32**, 4834 (1993).

37 M. Mikuriya, K. Minowa, and R. Nukada, *Bull. Chem. Soc. Jpn.*, **75**, 2595 (2002).

38 W. E. Hatfield, "Theory and Applications of Molecular Paramagnetism," ed by E. A. Boudreaux and L. N. Mulay, Wiley-Interscience, New York (1976).

39 Crystal data for **2**: $C_{14}H_{26}CuN_2O_{10}S_2$, $M = 474.01$, orthorhombic, $a = 9.321(14)$ Å, $b = 30.41(4)$ Å, $c = 35.04(5)$ Å, $V = 9932(25)$ Å^3, $T = 293(2)$ K, space group F_{ddd} (No. 70), $Z = 16$, Final $R1[I > 2\sigma(I)] = 0.1390$, $wR2$ [all data] = 0.4178.

40 M. Mikuriya, H. Azuma, R. Nukada, and M. Handa, *Chem. Lett.*, **1999**, 57.

41 J. Lewis, Y. C. Lin, L. K. Royston, and R. C. Thompson, *J. Chem. Soc.*, **1965**, 6464.

42 Ortep-3 for Windows: L. J. Farrugia, *J. Appl. Cryst.*, **30**, 565 (1997).